TETRAHYDROBIOPTERIN OXIDATION AND REACTIVE OXYGEN SPECIES CONTRIBUTE TO H_2O_2-INDUCED ENDOTHELIAL NITRIC OXIDE SYNTHASE DYSFUNCTION

A Thesis

Presented to

The Academic Faculty

by

Beth Michelle Boulden

In Partial Fulfillment

of the Requirements for the Degree

Master of Science in Biomedical Engineering

Georgia Institute of Technology

August 2005

TETRAHYDROBIOPTERIN OXIDATION AND REACTIVE OXYGEN SPECIES CONTRIBUTE TO H_2O_2-INDUCED ENDOTHELIAL NITRIC OXIDE SYNTHASE DYSFUNCTION

Approved by:

Dr. Samuel C. Dudley, Jr., Advisor
Department of Biomedical Engineering/School of Medicine
Georgia Institute of Technology/Emory University

Dr. Hanjoong Jo
Department of Biomedical Engineering
Georgia Institute of Technology/Emory University

Dr. W. Robert Taylor
Department of Biomedical Engineering/School of Medicine
Georgia Institute of Technology/Emory University

Date Approved: April 22, 2005

ACKNOWLEDGMENTS

I would like to thank the Dudley lab—Sam Dudley, Jon Allen, Deborah DeWitt, Michael Fan, Alice Huang, Zhe Jiao, Vijay Kasi, David Kim, Arnold Pfahnl, Lisa Shang, David Simpson, Ruaa Al-Baldawi, Caelin Cubenas, Clegg Honeycutt, Alana Reed—for their technical help, encouragement, and friendship. Thanks to my committee for their help in planning experiments. Thanks to Debra Smith and the Jo lab for providing mouse aortic endothelial cells, to Sergey Dikalov and Louise McCann for their technical assistance, and to Charmaine O'Rourke and Donna Rouse for help with document formatting. Thanks to Jana, Andy, Stephanie, PJ, Suchi, Preeti, Brenda, Mili, Zack, Andrew, Drake, Laura, Kat, Clara, and Lori for keeping me sane through their friendship. Thanks to my parents, Mike and Susan Boulden, for constantly reminding me of their love and support, and for overusing the phrase “hang in there.” Thanks to the rest of my family—Emily, Sarah, Ma, Thomas, Grand Katy, and everybody else—for reminding me that there is life outside of lab.

TABLE OF CONTENTS

LIST OF TABLES

LIST OF FIGURES

LIST OF SYMBOLS

ANOVA	analysis of variance
ATP	adenosine triphosphate
BAECs	bovine aortic endothelial cells
BH_2	7,8-dihydrobiopterin
BH_4	(6*R*)-5,6,7,8-tetrahydro-L-biopterin
CaM	calmodulin
cAMP	cyclic adenosine monophosphate
DOCA	deoxycorticosterone acetate
GTP	guanosine triphosphate
FAD	flavin-adenine dinucleotide
FMN	flavin mononucleotide
H_2O_2	hydrogen peroxide
MAECs	mouse aortic endothelial cells
MEK/ERK1/2	mitogen-activated protein kinase kinase/extracellular signal-regulated kinase ½
NADPH	reduced nicotinamide adenine dinucleotide phosphate
NO•	nitric oxide
$O_2^{\bullet-}$	superoxide
•OH	hydroxyl radical
$ONOO^-$	peroxynitrite
o-PD	o-phenylene diamine
PBS	phosphate buffered saline
PEG-SOD	polyethelene glycol conjugated superoxide dismutase
PI3K	phosphatidylinositol-3-kinase

PKA	protein kinase A
ROS	reactive oxygen species
SEM	standard error mean
SOD	superoxide dismutase
VEGF	vascular endothelial growth factor

SUMMARY

An oxidative stress in the form of H_2O_2 exposure previously has been shown to cause a transient increase in NO• production and a chronic increase in eNOS protein levels, presumably compensatory responses. Nevertheless, oxidative stress can cause an uncoupling of catalytic activity resulting in decreased NO• and increased $O_2^{\bullet-}$ production from eNOS. This uncoupling seems to be mediated predominantly by oxidation of tetrahydrobiopterin (BH_4), an eNOS required cofactor. To study how these phenomena regulate the physiological balance of reactive oxygen species (ROS), H_2O_2-induced NO• production was measured in endothelial cells using an NO• specific electrode. Following H_2O_2 exposure, NO• concentrations initially increased; however, if cells were challenged a second time with H_2O_2, the increase in NO• production was attenuated. We postulated that the decline in NO• production after H_2O_2 exposure resulted from BH_4 oxidation. This was tested by supplementing cells with BH_4 just prior to the second H_2O_2 exposure. BH_4 supplementation prevented the decrement in NO• production after a second H_2O_2 exposure.

Because H_2O_2 also activates NADPH oxidases, causing increased superoxide ($O_2^{\bullet-}$) production, we then postulated that BH_4 oxidation might be the result of a H_2O_2-induced increase in $O_2^{\bullet-}$. This was tested by supplementing cell media with the $O_2^{\bullet-}$ scavenger, polyethelene glycol conjugated superoxide dismutase (PEG-SOD), or with the NADPH oxidase inhibitor, apocynin. Results were supported with measurement of H_2O_2-induced NO• production in $p47^{phox}$-knockout cells, which have genetically inhibited NADPH oxidase. These manipulations, expected to reduce $O_2^{\bullet-}$, resulted in a recovery of NO• production, consistent with the idea that $O_2^{\bullet-}$ produced by NADPH oxidase lead to the reduced eNOS function upon a second H_2O_2 exposure through oxidation of BH_4.

Because peroxynitrite ($ONOO^-$) and hydroxyl radicals (•OH) can be produced from $O_2^{\bullet-}$ and are more potent oxidizers of BH_4, we tested whether either of these free radicals were involved in reduction of H_2O_2-induced NO• production with repetitive stimuli. Scavenging $ONOO^-$ with uric acid resulted in a full recovery of NO• production, and scavenging •OH with mannitol resulted in a partial recovery of NO• production. This suggested possible roles for both radicals in the reduction in H_2O_2-induced NO• release with multiple exposures.

In summary, repeated exposures to H_2O_2 resulted in declines in induced NO• production in BAECs. This reduction in the presumed compensatory NO• release could be attenuated by BH_4 supplementation, by scavengers of $O_2^{\bullet-}$, $ONOO^-$, and •OH, and by inhibition of the NADPH oxidase system. Therefore, uncoupled eNOS as a result of BH_4 oxidation may explain the failure of compensatory NO• release to repeated oxidative stresses. BH_4 supplementation or NADPH oxidase inhibition may be corrective in this condition.

CHAPTER 1

INTRODUCTION

1.1 The Importance of Oxidative Stress

Oxidative stress has been shown to contribute to several cardiovascular diseases, including hypertension, atherosclerosis, diabetes, ischemia-reperfusion injury, heart failure, restenosis, atrial fibrillation, and hypercholesterolemia[1, 2]. However, some oxidative stress, such as that produced in moderate exercise, is associated with decreased risk of cardiovascular disease[3-5]. Here, we explore one possible explanation that might lead to failure of the compensatory mechanism to deal with increased oxidative stress and the associated progression of disease states.

Many cardiovascular diseases are thought to be caused or perpetuated by an imbalance of reactive oxygen species (ROS), particularly superoxide ($O_2^{\bullet-}$) and nitric oxide (NO•)[2]. NO• is responsible for a wide range of beneficial cardiovascular functions, including vasodilation, decreased thrombosis formation, inhibition of fibroblast proliferation, reduced cell adhesion to endothelium, and increased myocardial lusitropy[6]. NO• is produced in endothelial cells primarily by endothelial nitric oxide synthase (eNOS). Changes in endothelial cell NO• levels can be caused either by changes in NO• production or by NO· degradation, as happens when it reacts with $O_2^{\bullet-}$ to form peroxynitrite ($ONOO^-$).

Efficient production of NO• by eNOS requires electron donation from the cofactor tetrahydrobiopterin (BH_4). If BH_4 is oxidized, electron transfer in eNOS becomes uncoupled, and eNOS produces $O_2^{\bullet-}$ instead of NO•[7]. This can have a significant effect on the bioavailability of NO•, since eNOS uncoupling reduces NO• production and might

increase NO• degradation by producing more $O_2^{\bullet-}$[8]. Because BH_4 can be oxidized easily by ROS prevalent in endothelial cells[8, 9], it is possible that BH_4 oxidation may be a feature of many cardiovascular disease states.

Hydrogen peroxide (H_2O_2) is the most stable and long-lasting ROS. Therefore, it can act as a paracrine signaling molecule[10]. H_2O_2 is known to activate both eNOS[11] and $O_2^{\bullet-}$-producing NADPH oxidase[10], so this membrane permeable ROS may be important in balancing the oxidative state of the cell. Previously, we have shown that a single exposure to H_2O_2 activates eNOS[11]. In these experiments, we explore whether this effect is maintained with multiple H_2O_2 challenges or if continued oxidative stress diminishes the presumably compensatory NO• release.

1.2 Specific Aims

Although some oxidative stress, such as that experienced during moderate exercise, has been shown to be beneficial, larger amounts of oxidative stress are thought to contribute to the development of cardiovascular disease. An understanding of this apparent paradox requires a deeper study of the delicate physiological balance between ROS, including $O_2^{\bullet-}$, H_2O_2, •OH, NO•, and $ONOO^-$. The overall aim of this project is to study this balance by examining the effect of H_2O_2, the most stable and long-lasting ROS, on production of NO• in endothelial cells.

Previous studies have shown that H_2O_2 causes an initial activation of endothelial nitric oxide synthase (eNOS)[11]. Nevertheless, we observed that if cells are challenged a second time with H_2O_2, the increase in NO• production is attenuated. The objective of this project was to determine the cause of NO• production attenuation after a second H_2O_2 exposure. We tested the hypothesis that the decline might be the result of uncoupled eNOS occurring with oxidation of the essential eNOS cofactor tetrahydrobiopterin (BH_4). The project consisted of three specific aims: (1) to determine

the role of BH_4 oxidation in H_2O_2-induced NO• production decline, (2) to determine which oxidizing agents might contribute to eNOS dysfunction, and (3) to evaluate role of NADPH oxidase in this dysfunction.

CHAPTER 2

ELECTROCHEMICAL DETECTION OF NITRIC OXIDE

2.1 Introduction

Electrochemical detection of nitric oxide (NO•) has certain advantageous characteristics including temporal resolution, spatial resolution, and sensitivity with a detection limit sufficient for biological samples[12, 13]. In this technique, the voltage is controlled so that NO• oxidation is catalyzed on an electrode surface. At a chosen sampling time and at a voltage above the redox potential of NO•, the current generated is a linear function of NO• concentration at the electrode surface. There are two common recording modes, cyclic voltammetry and amperometry. In cyclic voltammetry, voltage is varied and current is measured. This mode is best for identification of species, since the voltage corresponding to an increase in faradic current is determined by the half-cell potential specific to a particular chemical species (figure 2-1). In amperometry, voltage is held constant above the oxidation potential, and current is measured. This mode is used commonly to quantify species concentration. Electrodes are typically filaments made of carbon or platinum[13, 14]. They are made more specific by coatings that either attract NO•[15] or exclude other oxidizable species[16].

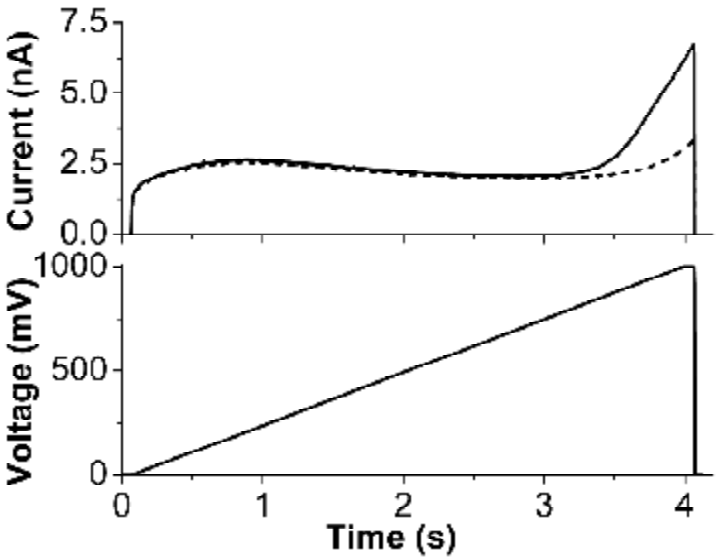

Figure 2-1: Voltammetry showing faradic current generated by NO•. The dashed line shows current elicited by the voltage ramp in phosphate buffered saline (PBS) only. With NO• present in solution, an additional, faradic current representing the oxidation of NO• can be seen at voltages above ~+750 mV relative to an AgCl reference electrode.

Here, we describe procedures for measuring NO• from endothelial cells and cardiac tissue using a carbon fiber electrode coated with Nafion and o-phenylenediamine (o-PD) exclusion coatings. The use of these exclusionary coatings was first described by Friedemann, et al[16]. Although other electrodes are available, even commercially, we have chosen this electrode because of its small tip size, ease of fabrication, reliability, and low cost.

2.2 Electrode Fabrication and Characterization

Electrodes were fabricated as described previously[16], with a few simplifications. Suitable Nafion-coated carbon electrodes (30 μm diameter and 100 μM exposed surface height) were purchased commercially (World Precision Instruments, Inc., Sarasota, FL). Electrode integrity was confirmed by voltage ramp protocols and by visual inspection

under a microscope (figure 2-2). About 70% of the electrodes purchased were suitable for experiments.

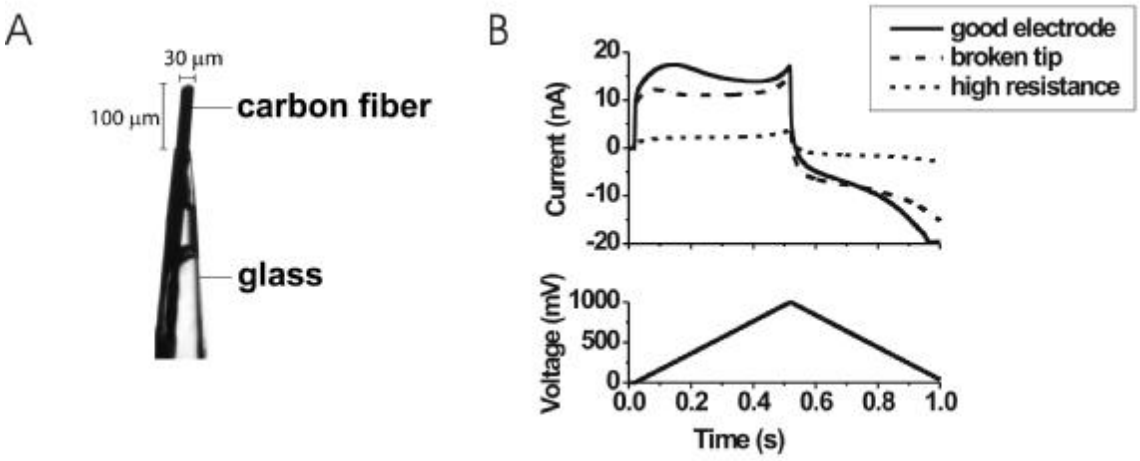

Figure 2-2: Evaluating electrode integrity. (A) Glass-encased, cylindrical carbon fiber electrode (30 ㎜m x 100 ㎜m exposed area). (B) Current responses in PBS to voltage ramp protocols to test electrode properties. High resistance electrodes are less sensitive to NO• and other oxidizable species. Electrodes with broken tips have current responses that tend to increase more quickly at higher increasing voltages than current responses for unbroken electrodes exposed to the same voltage ramp protocol.

After electrode integrity is confirmed, an additional o-phenylene diamine (o-PD) coating was applied to increase NO• specificity. o-PD was polymerized on the electrode surface at +900 mV in a stirred 5 mM o-PD solution at 37ºC for 45 min. The o-PD solution was made fresh by dissolving one tablet o-phenylenediamine dihydrochloride (3 mg substrate/tablet, Sigma, St. Louis, MO) in 3.3 mL of 100 µM ascorbic acid in 0.1 M phosphate buffered saline (PBS). Successful coating blocked ascorbic acid from the electrode, as is indicated by a significant decrease in current (from about 20 nA to 200 pA). After coating, the electrode was allowed to dry for about one minute, dipped in water, and then allowed to dry overnight. Electrodes were stored at 4ºC and could be used for several weeks after coating. Before each experiment, electrodes were hydrated by soaking in PBS for at least 1 hour to increase baseline electrical stability.

This form of exclusionary coating resulted in electrodes that were relatively selective for NO• when compared with other biological species with oxidation potentials in this range, such as H_2O_2, $O_2^{\bullet-}$, and ascorbic acid (table 2-1). To increase measurement accuracy in cells and tissue, the NO• synthase inhibitor, N_ω-Nitro-L-arginine methyl ester (L-NAME) was added during measurements, and the L-NAME suppressible current used to calculate the NO• concentration.

Table 2-1: Sensitivity of One Electrode to Various Oxidizable Species

Species	Electrode Sensitivity to Species (pA/nM)	NO• Sensitivity: Species Sensitivity
NO•	$5.5x10^{-2}$	1
Ascorbic Acid	$5.0x10^{-4}$	$9.1x10^{-3}$
H_2O_2	$1.7x10^{-3}$	$3.1x10^{-2}$
$O_2^{\bullet-}$	$7.0x10^{-4}$	$1.3x10^{-2}$

2.3 Electrode Data Acquisition and Analysis

To minimize mechanical vibrations that generate piezoelectric currents and ambient electrical noise detection, experiments were performed on a vibration isolation table and in a grounded Faraday cage. Measurements were taken relative to an AgCl reference electrode, and further noise reduction was accomplished by low-pass filtering with a 2 Hz cutoff frequency.

Because sensitivity of the electrode to NO• varied over time and between electrodes, each electrode was calibrated before each experiment. This was done by using dilutions of a saturated NO• solution. A stock solution of saturated NO• was produced by bubbling NO• gas through deionized water that had been deoxygenated using N_2 bubbling for 30 min. Immediately after saturation, a NO• solution at 20ºC has a concentration of 2 mM[17]. In a sealed system on ice, the solution NO• concentration stabilized at 1.4 mM over a 20 min period. An expedient method of calibration was

developed that involved serial additions of increasing volumes of diluted NO• solution added to deoxygenated 37ºC 0.1 M PBS while the electrode voltage was held constant at a voltage exceeding the NO• oxidation potential of +700 mV relative to a AgCl reference electrode (figure 2-3).

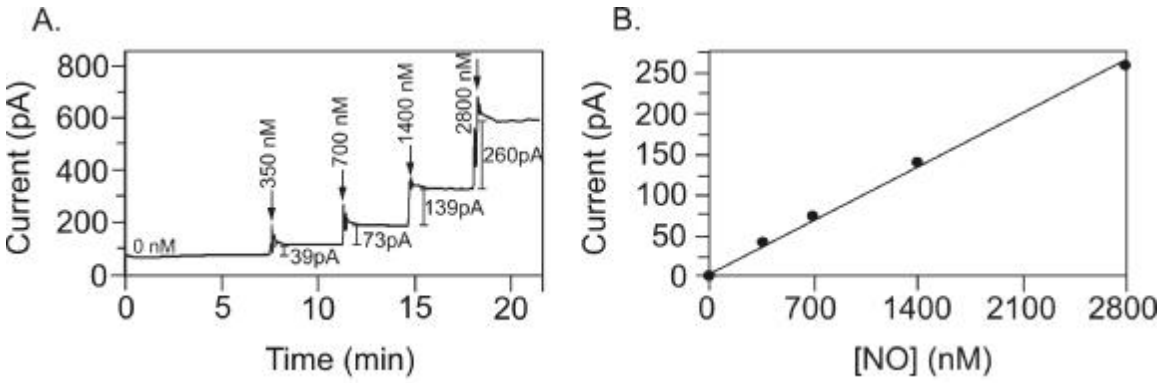

Figure 2-3: Electrode Calibration. (A) Serial additions of a concentrated solution of NO• are added and current recorded to create a calibration curve. (B) Using a cylindrical Nafion and o-PD coated carbon fiber electrode (30 ㎜ x 100 ㎜ exposed area) and a voltage of +900 mV, the detection limit is ~10 nM, and the response is linear up to 4 µM. The sensitivity from this calibration curve is 0.095 pA/nM, with R^2 = 0.996.

2.4 Measuring NO• from Endothelial Cells

NO• was originally known as endothelium derived relaxing factor[18, 19], and it is frequently desirable to measure NO• released from cultured endothelial cells under a variety of conditions. Electrodes are sufficiently sensitive to measure NO• from single endothelial cells[15], but we have generally measured from cultured monolayers of 60-90% confluency. To help minimize signal contamination, immediately prior to measurement, culture media was exchanged with warmed 0.1 M PBS (pH 7.4). With the dish of cells placed in a temperature controller on an inverted microscope stage, the electrode was positioned carefully using a micromanipulator. Baseline current measurements were made with the electrode voltage held at +900 mV and when the electrode was 5 µm

away from the cells. The NO• concentration gradient falls off as a function of distance from the cells, so the electrode was placed at a consistent distance above the monolayer. After positioning near cells, the current increase from baseline was recorded. The L-NAME suppressible signal was taken as indicative of the NO• faradic current and was converted to a NO• concentration (see figure 3-1 in chapter 3). For most cell experiments, chemicals were added to cells to determine their effect on NO• production. For each chemical, control experiments were performed to ensure that the chemical did not interfere with the faradic current.

2.5 Measuring NO• from Cardiac Tissue

Others and we have shown that in healthy heart, most NO• is produced by the endocardium[20, 21]. Pathological states can alter endocardial NO• production. We attempted to measure endocardial NO• from pig or mouse hearts under various experimental conditions. Harvested tissue was rinsed in oxygenated Krebs-HEPES buffer (in mmol/L, NaCl 99.01, KCl 4.69, $CaCl_2$ 1.87, $MgSO_4$ 1.20, K_2HPO_4 1.03, Na-NHEPES 20, and D-glucose 11.1) and stored on ice. Tissue showed no deterioration in NO• production under these conditions for several hours.

In general, NO• measurements from tissue were similar to measurements from cultured cells. Measurements were made at 37ºC from trimmed myocardial pieces secured with pins in silicone-coated dishes. Several challenges made NO• measurements from tissue more difficult than measurements from cells. The distance between the tissue and the electrode was more difficult to determine than in cells. To position the electrode, tissue deformation was observed in a stereomicroscope. Then, the electrode was backed away from the tissue a fixed distance. If the electrode was not precisely positioned above the tissue, piezoelectric currents developed due to carbon fiber bending. These were considerably larger than the true faradic current. Finally,

spatial heterogeneity of NO• production was evident. In the ventricular endocardium of mice, NO• production tended to increase toward the apex of the heart. Variations over smaller regions were also noted. Despite these difficulties, an L-NAME suppressible current could be measured from tissue (figure 2-4). Nevertheless, the remainder of this thesis focused on measurements of NO• from endothelial cell cultures.

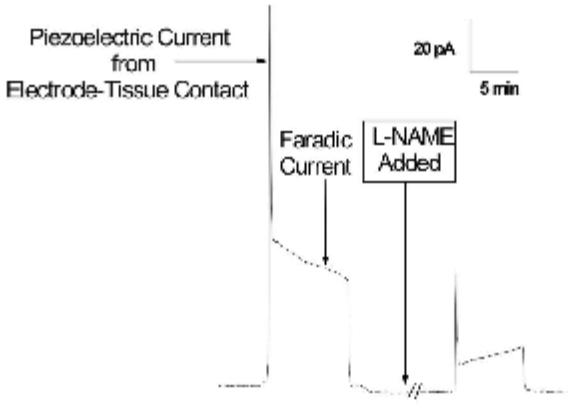

Figure 2-4: NO• signal from the endocardium is L-NAME suppressible. The electrode was placed in Krebs-HEPES bath far from the tissue, and lowered onto the tissue, resulting in a piezoelectric current. Then, the electrode was removed a fixed distance from the tissue, the faradic current was measured, and the electrode was removed from proximity to the endocardial surface, resulting in the reduction of faradic current to baseline. This procedure was repeated after the addition of L-NAME, showing that most of the faradic current from endocardial cells could be ascribed to NO•.

2.6 Conclusion

In conclusion, electrochemistry can be used to reliably measure NO• produced by endothelium or endocardium. The method is desirable because of its spatial and temporal resolution. We have developed methods for measuring NO• concentration in endothelial cells and cardiac tissue using Nafion and o-PD carbon fiber electrodes. These techniques can also be applied to other tissues, and alterations in the electrode design have allowed use of electrochemistry to detect other biologically relevant molecules such as $O_2^{\bullet-}$ and H_2O_2[22, 23].

CHAPTER 3

PREVENTION OF A DECLINE IN H_2O_2-INDUCED ENDOTHELIAL CELL NITRIC OXIDE PRODUCTION BY TETRAHYDROBIOPTERIN, ROS SCAVENGERS, AND NADPH OXIDASE INHIBITION

3.1 Abstract

An oxidative stress in the form of H_2O_2 exposure previously has been shown to cause a transient increase in NO• production and a chronic increase in eNOS protein levels. Nevertheless, oxidative stress can cause an uncoupling of catalytic activity resulting in decreased NO• and increased $O_2^{\bullet-}$ production from eNOS. This uncoupling seems to be mediated predominantly by oxidation of tetrahydrobiopterin (BH_4), an eNOS required cofactor. To study how these phenomena regulate the physiological balance of reactive oxygen species (ROS), H_2O_2-induced NO• production was measured in bovine aortic endothelial cells (BAECs) using an NO• specific electrode. Following H_2O_2 exposure, NO• concentrations initially increased; however, if cells were challenged a second time with H_2O_2, the increase in NO• production was attenuated. We postulated that the decline in NO• production after H_2O_2 exposure resulted from BH_4 oxidation and tested this by supplementing cells with BH_4 prior to the second H_2O_2 exposure. This resulted in a recovery of NO• production. Since H_2O_2 also activates NADPH oxidase to produce superoxide ($O_2^{\bullet-}$), we tested whether the decrease in NO• production during the second H_2O_2 exposure could be explained by increased NADPH oxidase-dependent oxygen free radical production, including $O_2^{\bullet-}$, peroxynitrite ($ONOO^-$), and hydroxyl radicals (•OH). A reduction in H_2O_2-induced NO• release was prevented in apocynin- and PEG-SOD-treated cells and in $p47^{phox}$-knockout mouse aortic endothelial cells (MAECS), which lack a critical subunit of the NADPH oxidase. These results suggest

that $O_2^{\bullet-}$ produced by NADPH oxidase leads to eNOS dysfunction. Scavenging $ONOO^-$ resulted in a full recovery of NO• production, and scavenging •OH resulted in a partial recovery of NO• production. This implies roles for these $O_2^{\bullet-}$ derivatives in the reduced NO• response to repeated H_2O_2 exposures.

3.2 Background and Significance

3.2.1 Oxidative Balance

Oxidative stress has been shown to contribute to several cardiovascular diseases; however, some oxidative stress, such as that produced in moderate exercise, is associated with decreased risk of cardiovascular disease[3-5]. One possible explanation for this apparent paradox is that a small amount of oxidative stress increases the oxidative buffering capacity of the body, while a larger amount overpowers the compensatory mechanism. In these experiments, we explore one possible explanation for the failure of that compensatory mechanism.

Many cardiovascular diseases are thought to be caused or perpetuated by an imbalance of reactive oxygen species (ROS), particularly superoxide ($O_2^{\bullet-}$) and nitric oxide (NO•)[2]. NO• is produced throughout the body by endothelial nitric oxide synthase (eNOS), neuronal nitric oxide synthase (nNOS) and inducible nitric oxide synthase (iNOS) and is responsible for a wide range of beneficial cardiovascular functions. In the cardiovascular system under physiological conditions, NO• is produced primarily by eNOS. $O_2^{\bullet-}$ is produced by xanthine oxidase, mitochondria, NADPH oxidase, cytochrome P450, cyclooxygenase, and uncoupled eNOS. $O_2^{\bullet-}$ reacts quickly with NO• to form $ONOO^-$ or is dismutated by superoxide dismutase (SOD) to H_2O_2[24, 25].

3.2.2 eNOS Structure and Function

eNOS is a homodimeric enzyme, with each subunit containing an oxygenase domain, which binds heme, tetrahydrobiopterin (BH_4), and L-arginine; a reductase

domain, which binds flavoproteins FAD, FMN, and NADPH; and a calmodulin (CaM)-binding domain, which connects the oxygenase and reductase domains[26]. NO• is produced when eNOS converts L-arginine to N^{ω}-hydroxyl-L-arginine and then to L-citrulline and NO•. This involves a two-electron transfer to the eNOS heme.

In order for eNOS to be activated, it must be optimally aligned for efficient electron transfer. This requires conformational changes through binding of calcium-dependent calmodulin (CaM) and through phosphorylation of several serines on eNOS[27]. Serine phosphorylation occurs via two primary pathways: phosphatidylinositol-3-kinase (PI3K) activation of Akt[28] or adenylate cyclase activation of protein kinase A (PKA) through production of cAMP[29]. The Akt pathway can be activated by shear stress (via G proteins)[30], vascular endothelial growth factor (VEGF)[31], insulin-like growth factor[30], sphingosine-1-phosphate[32], estrogen[33], and H_2O_2[11]. The PKA pathway can be activated by shear stress (via G proteins)[30], VEGF[30], and bradykinin[34]. H_2O_2 also activates eNOS through phosphorylation by the MAP kinase kinase MEK/ERK1/2 pathway[11]. VEGF, estrogen, sphingosine-1-phosphate, and bradykinin simultaneously activate phospholipase C-γ, which facilitates Ca^{++} release from the endoplasmic reticulum, promoting binding of CaM to eNOS[27] and increasing eNOS activation.

The first of the two electrons required for NO• production is donated by an NADPH molecule and transferred via two flavin molecules (FAD and FMN) to the heme oxygen[26]. The second electron can come from the reductase domain or from BH_4[7]. A heme oxygen that has been activated by one electron is unstable; if another electron is not readily available, this oxygen can be released as $O_2^{\bullet -}$[7]. Electron donation by BH_4 is faster than donation by the reductase domain. Therefore, if BH_4 is oxidized or unavailable, eNOS tends to produce $O_2^{\bullet -}$ instead of NO•[35]. This phenomena is referred to as eNOS uncoupling[36].

3.2.3 Tetrahydrobiopterin

BH_4 is involved not only in NO• production as a cofactor of nitric oxide synthases, but also in phenylalanine metabolism as a cofactor of phenylalanine hydroxylase[37] and in neurotransmitter synthesis[38]. BH_4 is produced *de novo* from GTP by three enzymes: GTP cyclohydrolase I (GTPCH), 6-pyruvoyl-tetrahydrobiopterin synthase, and sepiapterin reductase[39]. Production of the intermediate dihydroneopterin triphosphate by GTPCH is the rate limiting step, and much of the control of BH_4 synthesis is thought to occur through GTPCH[40]. GTPCH is transcriptionally controlled by interferon γ, tumor necrosis factor α, lipopolysaccharide, and insulin[41]. GTPCH activation is controlled primarily by the GTPCH feedback regulatory protein (GFRP), which allows for negative feedback by BH_4[42]. BH_4 can also be produced via a "salvage" pathway, in which sepiapterin is converted with sepiapterin reductase to 7,8-dihydrobiopterin (BH_2), which is then converted to BH_4 with dihydrofolate reductase[43]. Although production of sepiapterin in mammalian cells has not been well characterized, this pathway has been used in the lab to increase cellular BH_4 levels[8, 44].

In eNOS, BH_4 donates an electron to become a protonated trihydrobiopterin cation (BH_3•H^+). It is then reduced to BH_4 again by an electron from the eNOS reductase domain. Steady replacement of BH_4 is therefore not necessary in endothelial cells, unless BH_4 is depleted by oxidation[41].

BH_4 can be oxidized by several ROS, including $O_2^{\bullet-}$, $ONOO^-$ [8], and hydroxyl radicals (•OH)[9, 45], all of which are prevalent in endothelial cells. $O_2^{\bullet-}$ is produced in endothelial cells by NADPH oxidase, xanthine oxidase, uncoupled eNOS, mitochondria, cytochrome P450, and cyclooxygenase[46, 47]. $ONOO^-$ comes from a reaction between NO• and $O_2^{\bullet-}$, and $ONOO^-$ levels can increase in a cell due to an increase in NO• production, an increase in $O_2^{\bullet-}$ production, or a combination of the two. Hydroxyl radicals (•OH) can come from several sources, including degradation of protonated $ONOO^-$, the

Fenton reaction ($Fe^{2+} + H_2O_2$ **à** $Fe^{3+} + \bullet OH + OH^-$), or in small amounts by the Haber-Weiss reaction ([$H_2O_2 + O_2^{\bullet-}$ **à** $O_2^{\bullet-} + OH^- + \bullet OH$])[46, 48, 49].

3.2.4 NADPH Oxidases

$O_2^{\bullet-}$, $ONOO^-$, and •OH are all formed when production of $O_2^{\bullet-}$ increases. The NADPH oxidases are a major source of $O_2^{\bullet-}$ in endothelial cells[24, 50]. The endothelial cell NADPH oxidases are composed of several subunits, including membrane proteins $p22^{phox}$ and $gp91^{phox}$ (or $gp91^{phox}$-like proteins NOX1, NOX4, or NOX5), along with cytoplasmic proteins Rac, $p40^{phox}$, $p67^{phox}$, and $p47^{phox}$ [10, 50]. Activation of the NADPH oxidases is dependent on phosphorylation of $p47^{phox}$, which allows binding of $p47^{phox}$ to the $p22^{phox}$ subunit[51]. The NADPH oxidases are activated in a variety of ways, including by mechanical forces, hormones such as angiotensin II, and H_2O_2[10]. Apocynin is a specific NADPH oxidase inhibitor that works by preventing NADPH oxidase subunit assembly[52].

3.2.5 H_2O_2, eNOS, and NADPH Oxidases

H_2O_2, most commonly produced when $O_2^{\bullet-}$ is dismutated by superoxide dismutase (SOD), is the most stable and long lasting of the reactive oxygen species. It is likely to play a critical role in maintaining the balance between $O_2^{\bullet-}$ and NO•, since it has been shown to act as a signaling molecule for both NADPH oxidases and eNOS.

H_2O_2 activates the NADPH oxidases by stimulating signaling protein c-Src, which phosphorylates the NADPH oxidase subunit $p47^{phox}$, allowing $p47^{phox}$ to move to the cell membrane and bind to the $p22^{phox}$ subunit[10]. H_2O_2 activation of NADPH oxidase provides a form of positive feedback—a small amount of $O_2^{\bullet-}$ is produced and dismutated to H_2O_2, which activates additional production of $O_2^{\bullet-}$.

H_2O_2 has been shown also to act as a signaling molecule for eNOS upregulation and activation. Exposure of endothelial cells to H_2O_2 causes upregulation of eNOS after several hours[53]. On a shorter time scale (several min), H_2O_2 activates eNOS through

phosphorylation[11]. Both of these processes would seem to help maintain a compensated, balanced redox state in the face of increased oxidative stress. However, continued exposure to H_2O_2 for an intermediate time period (30 min) causes an initial increase in NO• production followed by a decline in NO• production[54, 55]. One mechanism of this decline in NO• production may be eNOS uncoupling in the continued presence of an oxidative stress.

3.3 Materials and Methods

3.3.1 Cell Culture

Bovine aortic endothelial cells (BAECs) (Cell Systems, Kirkland, WA) were cultured on 0.05% gelatin using M199 media (Cellgro, Herndon, VA) containing 10% FCS (Hyclone, Logan, UT) and 1% of each of the following: penicillin/streptomycin (Cellgro), MEM vitamins (Cellgro), L-glutamine (Invitrogen-Gibco, Carlsbad, CA), and MEM Amino Acids (Invitrogen-Gibco). Experiments were performed at 37ºC on passage 4 or 5 cells that were 60-90% confluent.

$p47^{phox}$-knockout and wild type mouse aortic endothelial cells (MAECs) were obtained from Dr. Hanjoong Jo. Cells were isolated as described previously[56] and cultured on 0.1% gelatin in DMEM (Invitrogen-Gibco) containing 1.25% MEM non-essential amino acids (Invitrogen-Gibco), 12.5% FBS (Atlanta Biologicals), 2.5 U/mL heparin (Baxter, Deerfield, IL), and 2% endothelial cell growth serum (isolated from bovine brain extract). Experiments were performed at 37ºC on passages 6-10 at 60-90% confluency.

3.3.2 NO• Measurement

NO• was measured using a carbon electrode coated for NO• selectivity with Nafion and o-phenylenediamine. Nafion-coated carbon electrodes (100 µm exposed length x 30 µm diameter) were obtained commercially (World Precision Instruments,

Sarasota, FL) and coated with o-phenylenediamine as described previously[16]. NO• was measured amperometrically against an AgCl reference electrode, with the voltage of the electrode held constant at +900 mV, above the oxidation potential of NO•. After calibration with known concentrations of NO• (obtained by bubbling NO• through N_2-degassed deionized H_2O to saturation), the electrode was carefully lowered to the cell surface using a micromanipulator, then backed away 5 µm. To insure the faradic current represented only NO• current seen in the presence of the eNOS inhibitor, L-NAME (N_ω-Nitro-L-arginine methyl ester, 2 mM) was subtracted from the unprocessed current to give the L-NAME suppressible current. All electrodes used showed linear calibration curves with $R^2 > 0.95$.

3.3.3 Cell Treatments

Prior to experiments, cells were incubated in 60 µM BH_4 for 10 min to compensate for BH_4 deficiencies known to occur in the oxidized environment of the cell culture incubator[57-59]. BH_4 was made fresh daily and used within several hours. After BH_4 incubation, cells were rinsed with PBS (pH 7.4, 37°C) to prevent BH_4 electrode interference. With cells in PBS media, the electrode was lowered to 5 µm above the cell, and current was measured until a stable baseline was achieved. Cells were then exposed to 50 µM H_2O_2, and the resulting increase in NO• production was measured for 30 min ("H_2O_2 exposure 1"). The same cells were rinsed again with PBS, and current was measured 5 µM above the cell until a stable baseline was achieved. The cells were again exposed to 50 µM H_2O_2 as the increase in NO• production was measured for 30 min ("H_2O_2 exposure 2").

To determine possible mediators of the NO• production decrease upon H_2O_2 exposure 2, cells were pre-incubated for 30 min with apocynin (600 µM), $O_2^{\bullet-}$ scavenger PEG-SOD (450 U/mL), $ONOO^-$ scavenger uric acid (100 µM), or •OH scavenger mannitol (3 mM) prior to the initial 10-minute BH_4 incubation. To maximize their effects

but prevent any faradic contamination when measuring NO•, uric acid, mannitol, and apocynin treatments were extended into H_2O_2 exposure 1 but not H_2O_2 exposure 2. All chemicals were obtained from Sigma Chemicals (St. Louis, MO) unless otherwise noted.

3.3.4 Data Analysis

Data was obtained and analyzed using pClamp 8.0 (Axon Instruments, Union City, CA). Unprocessed currents were low-pass filtered using an 8-pole Bessel filter with cutoff frequency of 2 Hz. Statistical analysis was performed using Microsoft Excel (Redmond, WA) and Graphpad Prism (Graphpad Software, Inc., San Diego, CA). NO• production as a function of time in response to H_2O_2 was compared using two-way ANOVAs. Integrated NO• concentrations were compared using one-way ANOVAs or t tests with corrections for multiple comparisons as appropriate. A $p<0.05$ was considered to be statistically significant. All values are reported as mean ± SEM.

3.4 Results

3.4.1 NO• Production in Response to H_2O_2

The majority of the faradic current measured from BAECs after H_2O_2 exposure appeared to be eNOS-dependent NO• release. After BH_4 supplementation to insure complete eNOS loading in all experiments, BAECs showed an increase in faradic current in response to 50 μM H_2O_2 exposure. Most of the faradic current was suppressible by 2 mM L-NAME, suggesting that this signal was the result of NO• production (figure 3-1). In subsequent experiments, the L-NAME suppressible signal was used.

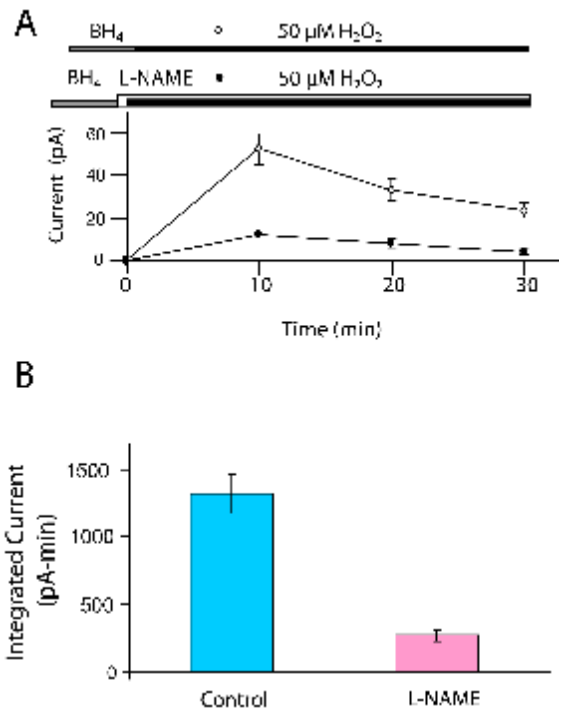

Figure 3-1: Determination of NO• concentration from the L-NAME suppressible faradic current. Panel A: Electrode responses to H_2O_2 in the presence and absence of the NOS inhibitor, L-NAME. The electrode is around 50 times more sensitive to NO• than H_2O_2, but the difference in concentrations results in a minimal faradic current in response to H_2O_2. Control experiments were performed by measuring current detected by the electrode upon addition to 50 μM H_2O_2 to BAECs preincubated for 10 min with 60 μM BH_4 (n=9). L-NAME experiments were performed by measuring current detected by the electrode in the presence of 2 mM L-NAME upon addition of 50 μM H_2O_2 to BAECs (n=11). Panel B: Seventy-nine percent of the integrated faradic current is suppressible by L-NAME. All subsequent results are reported as the L-NAME suppressible signal.

BAECs showed a reduction in NO• release upon a second exposure to H_2O_2. Cells exposed to 50 μM H_2O_2 following preincubation with 60 μM BH_4 (H_2O_2 exposure 1) increased NO• production after 10 min to 356 ± 94 nM (mean ± SEM, n=9). After 30 min, the NO• concentration decreased to 183 ± 51 nM. As an index of the total amount of NO• produced by cells, the integrated NO• signal over 30 min was 11261 ± 2193 nM·min. After cells were rinsed in PBS, they were again exposed to 50 μM H_2O_2 (H_2O_2 exposure 2). The amount of NO• produced during H_2O_2 exposure 2 was less than that produced during H_2O_2 exposure 1. During H_2O_2 exposure 2, NO• increased to 154 ± 49 nM (n=9) by 10 min and then declined to 109 ± 35 nM at 30 min and was significantly

reduced from that seen with H_2O_2 exposure 1 ($p<0.05$). The integrated NO• production over 30 min was 5402 ± 1109 nM·min, significantly reduced from the first exposure ($p<0.05$, figure 3-2).

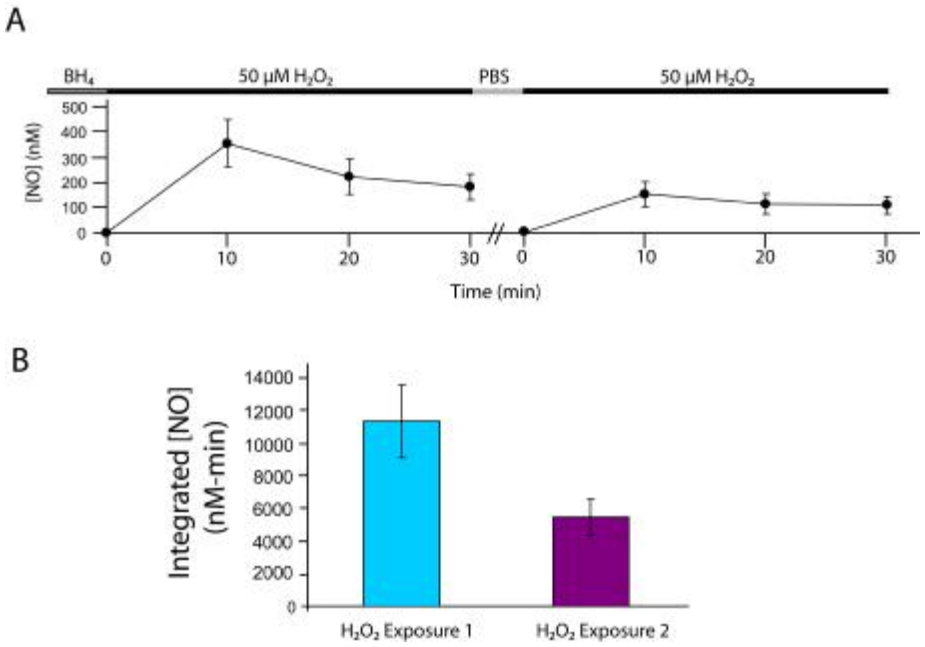

Figure 3-2: NO• induction by H_2O_2 is attenuated with multiple exposures. Panel A: Cells were incubated in 60 μM BH_4 for 10 min prior to experiments to compensate for BH_4 oxidation in cell culture. Following addition of 50 μM H_2O_2 to BAECs, NO• production increases (n=9). Subsequent addition of 50 μM H_2O_2 following PBS rinsing causes statistically smaller increases in NO• production (n=9; $p<0.05$). Panel B: Integrated NO• production over time, an index of total NO• produced, is statistically reduced during the second exposure to H_2O_2 as compared to the first exposure ($p<0.05$).

The decline in H_2O_2-mediated NO• release from BAECs was mitigated by addition of BH_4. Supplementing cells with 60 μM BH_4 prior to H_2O_2 exposure 2 prevented the decrease in NO• production (figure 3-3). Following a second supplementation, the H_2O_2 exposure 2-induced NO• concentration increased after 10 min to 407 ± 77 nM and declined by 30 min to 225 ± 53 nM. Integrated NO• production over 30 min was 11164 ± 1990 nM·min (n=4). Comparing either the time courses of NO• production or the integrated NO• values indicated that total NO• production from cells supplemented with BH_4 just prior to H_2O_2 exposure 2 was not statistically different from

NO• production during H_2O_2 exposure 1 (p=0.4 and p=0.7, respectively). The restoration of NO• production in response to a second application of H_2O_2 by BH_4 supplementation suggested that BH_4 oxidation may be responsible for the loss of eNOS synthetic function after repeated oxidant exposures.

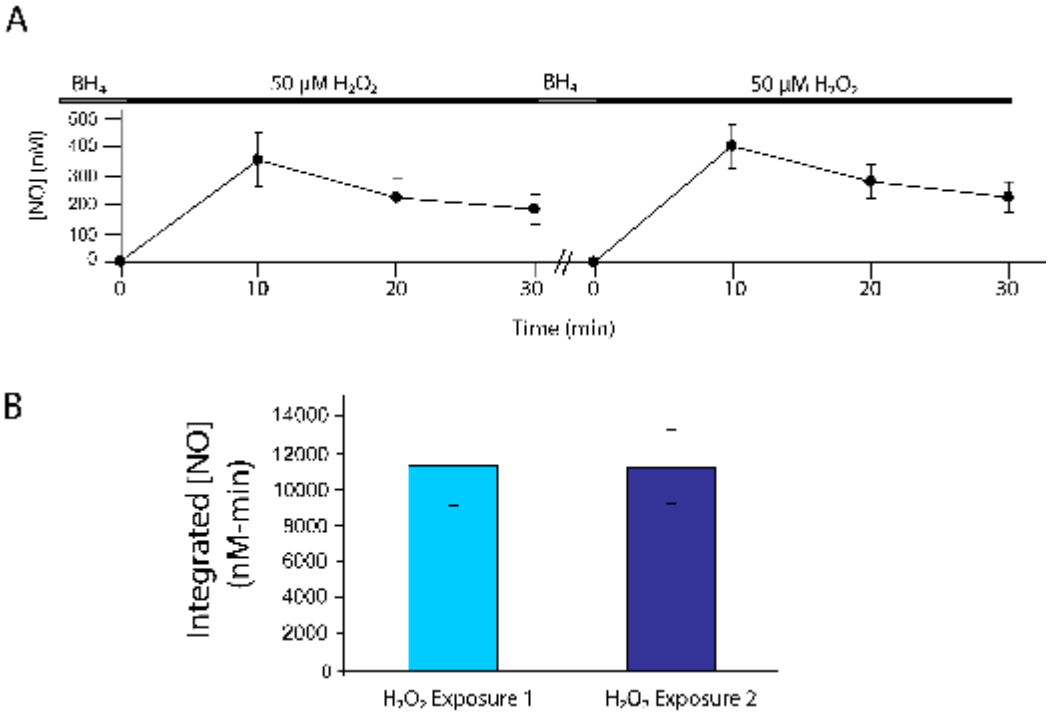

Figure 3-3: BH_4 prevents eNOS dysfunction upon multiple H_2O_2 exposures. Panel A: Replenishing BAECs with 60 µM BH_4 for 10 min prior to rechallenging cells with 50 µM H_2O_2 prevents the reduction in H_2O_2-induced NO• production seen with a second exposure to this ROS. In the case of BH_4 supplementation between exposures, the first and second NO• production responses to H_2O_2 are similar (p=0.4). Panel B: Integrated NO• production after exposure to H_2O_2 is statistically equivalent when cells are treated with BH_4 (1st exposure, n=9; 2nd exposure, n=4; p=0.7).

3.4.2 $O_2^{\bullet-}$ Scavenging Prevents the Loss of NO• Production with Repeated Exposures to H_2O_2

We tested the possibility that $O_2^{\bullet-}$ might contribute to eNOS dysfunction by using the cell permeable $O_2^{\bullet-}$ scavenger, PEG-SOD. Treating cells with PEG-SOD prevented the decreased NO• production seen during H_2O_2 exposure 2. The peak increase in NO• upon a second exposure to H_2O_2 after cells were incubated with PEG-SOD was 518 ± 91 nM at 10 min, and the NO• concentration declined to 400 ± 81 nM after 30 min. This

resulted in an integrated NO• production of 15662 ± 2754 nM·min (n=4) (figure 3-4). This NO• production after a second exposure to H_2O_2 in PEG-SOD-treated cells was statistically improved when compared to a second exposure response in the absence of treatment ($p<0.01$) and was similar to that seen with a second BH_4 supplementation treatment ($p=0.23$). This result suggested that $O_2^{\bullet-}$ was causing the resultant eNOS dysfunction after repeat exposures to H_2O_2, perhaps through BH_4 oxidation.

Because NADPH oxidases are activated by H_2O_2 and produce $O_2^{\bullet-}$ [50], we hypothesized that their increased activity may be responsible for the eNOS dysfunction seen on the second H_2O_2 exposure. Suggesting this is the case, inhibiting NADPH oxidase assembly with apocynin (600 µM) prevented the eNOS dysfunction. Upon H_2O_2 exposure 2, apocynin-treated cells produced 352 ± 119 nM NO• at 10 min that declined slightly by 30 min to 318 ± 78 nM (n=4). Integrated NO• over 30 min was 11003 ± 2406 nM·min. A comparison of integrated NO• values indicated that the integrated NO• produced by apocynin was statistically different from control ($p<0.05$), and that apocynin, BH_4, and PEG-SOD treatments resulted in indistinguishable salvage of NO• production after a second H_2O_2 treatment ($p=0.34$ by one-way ANOVA).

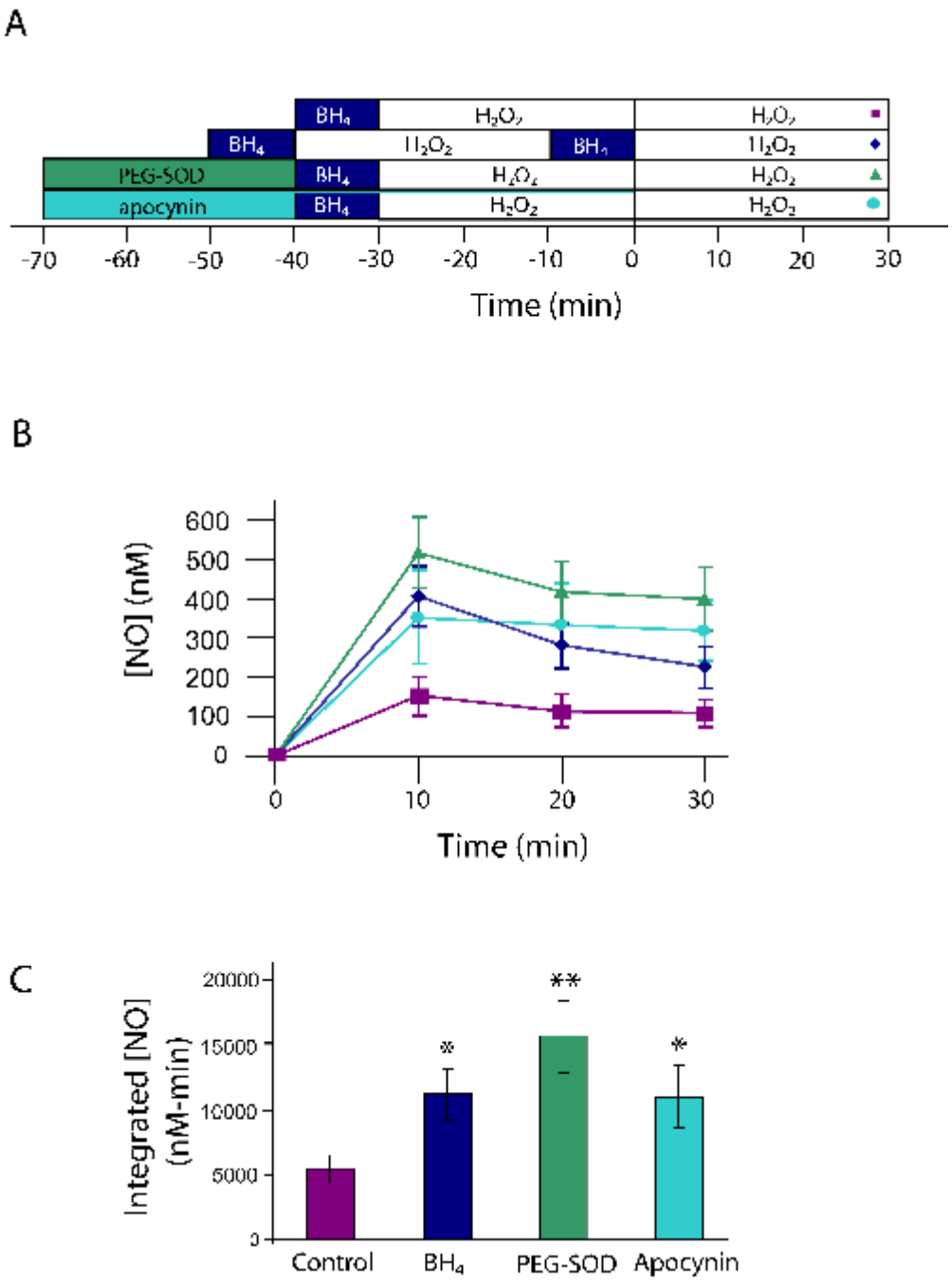

Figure 3-4: Superoxide scavenging and NADPH oxidase inhibition prevent a decrease in NO• production after multiple H_2O_2 additions. Panel A: Time course of treatments with BH_4 (60 µM), PEG-SOD (450 U/mL), apocynin (600 µM), and H_2O_2 (50 µM). Panel B: Comparison of NO• production during H_2O_2 exposure 2 with control (n=9, purple squares), BH_4 (n=4, blue diamonds), PEG-SOD (n=4, green triangles), and apocynin (n=4, aqua circles) treatments. Panel C: Integrated NO• production over 30 min. BH_4, PEG-SOD, and apocynin treatments were statistically different from control (= p<0.05, ** = p<0.01) but not from each other (p=0.34).*

To support results seen with chemical inhibition of NADPH oxidase, we repeated experiments in aortic endothelial cells isolated from $p47^{phox}$-knockout mice, lacking a critical subunit of the NADPH oxidase. Although there was a significant difference between H_2O_2 exposure 1 and H_2O_2 exposure 2 integrated NO• production in wild-type MAECs ($p<0.05$), NO• production was similar during both H_2O_2 exposures in $p47^{phox}$-knockout cells ($p=0.7$). In wild type cells, NO• production increased during H_2O_2 exposure 1 to 342±78 nM at 10 min and declined to 275±56 nM at 30 min, for an integrated NO• production of 10729±2075 nM·min (n=5). During H_2O_2 exposure 2, NO• production increased to 189±54 nM and declined to 110±22 nM after 30 min, and integrated NO• production over 30 min was 5135±1009 nM·min (n=9). This represented a 2.1 fold decrease in total NO• production during the second exposure. In $p47^{phox}$-knockout cells, NO• production increased to 409±182 at 10 min and decreased to 284±80 nM at 30 min during H_2O_2 exposure 1. Integrated NO• production over 30 min was 11568±1965 nM·min (n=4). A second challenge with H_2O_2 caused a similar increase to 435±128 nM at 10 min and 252±70 nM at 30 min, with an integrated NO• production of 10283±3208 (n=3) (figure 3-5), eliminating the reduction in NO• production seen in the wild type cells.

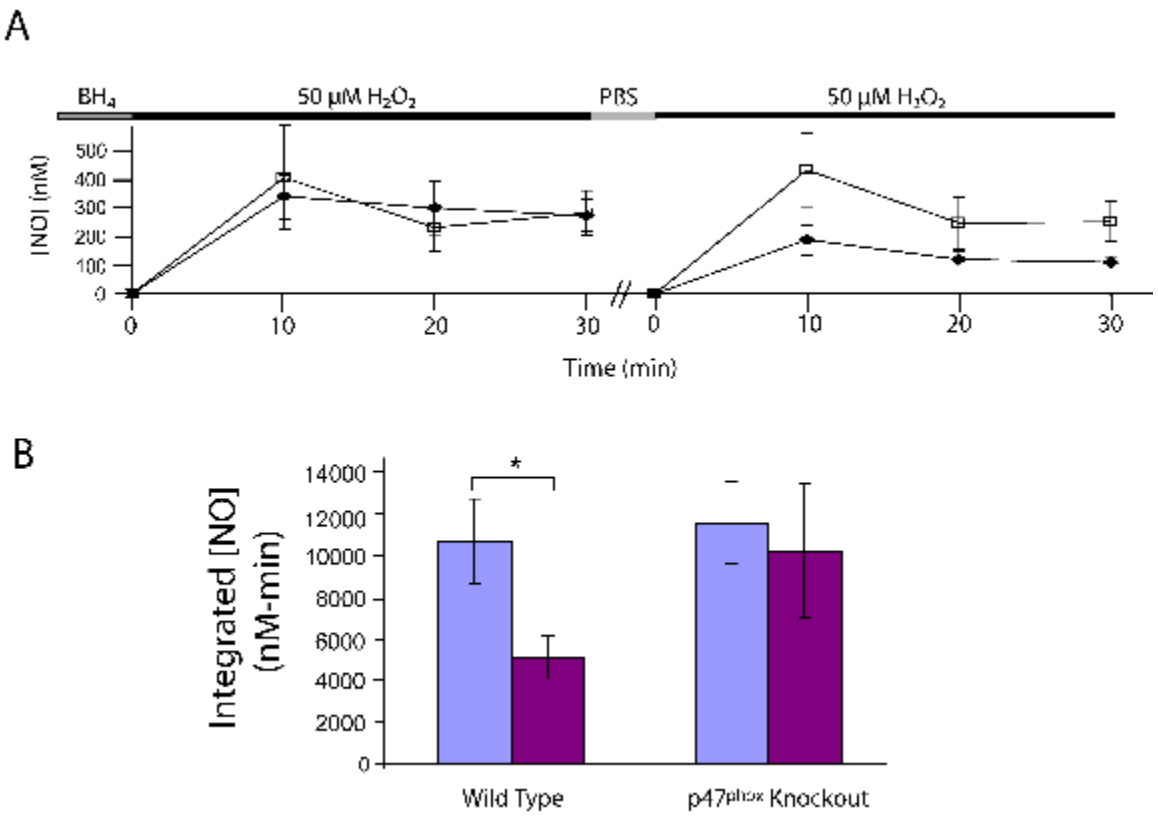

Figure 3-5: eNOS dysfunction with multiple H_2O_2 exposures is decreased in $p47^{phox}$-knockout MAECs. Panel A: Time course of NO• production in wild type (black diamonds) and $p47^{phox}$-knockout (white squares) MAECs in response to 50 μM H_2O_2 after preincubation for 10 min with 60 μM BH_4. NO• production during subsequent H_2O_2 exposures was statistically different in wild type cells (n=5 for H_2O_2 exposure 1, n=9 for H_2O_2 exposure 2, p<0.05) but not in knockout cells (n=4 for H_2O_2 exposure 1, n=3 for H_2O_2 exposure, 2, p=0.9). Panel B: Integrated NO• production over 30 min in wild type and $p47^{phox}$-knockout MAECs (H_2O_2 exposure 1, light purple, H_2O_2 exposure 2, dark purple). Integrated NO• production was statistically different in subsequent H_2O_2 exposures to wild type cells (= p<0.05) but not in knockout cells (p=0.7).*

3.4.3 ROS Scavengers Prevent the Loss of NO• Production with Repeated Exposures to H_2O_2

Production of $O_2^{\bullet-}$ also increases cellular levels of $ONOO^-$ and •OH, since $ONOO^-$ forms by reaction of $O_2^{\bullet-}$ with NO•, and •OH forms by degradation of protonated $ONOO^-$ or through the Haber-Weiss reaction[46, 49]. BH_4 is thought to be preferentially oxidized by these free radical species in comparison to $O_2^{\bullet-}$[8]. We sought to determine whether these species were playing a role in the reduced eNOS function seen with repeated H_2O_2 exposures. Treating cells with $ONOO^-$ scavenger, uric acid caused NO• production

during H_2O_2 exposure 2 to increase to 474 ± 96 nM by 10 min with a decline to 222 ± 43 nM by 30 min. The integrated NO• production was 11030 ± 2356 nM·min (n=4) (figure 3-6). This was statistically indistinguishable from the effect of BH_4 (p=0.65). Treating cells with the •OH scavenger, mannitol, had an intermediate effect, causing NO• production during H_2O_2 exposure 2 to increase at 10 min to 271±73 nM and to decrease by 30 min to 235±42 nM. The integrated NO• concentration with mannitol preincubation was 8250±1236 nM·min. The effect of mannitol was statistically indistinguishable from the control (p>0.05). However, the trend in NO• production suggested a partial recovery in NO•.

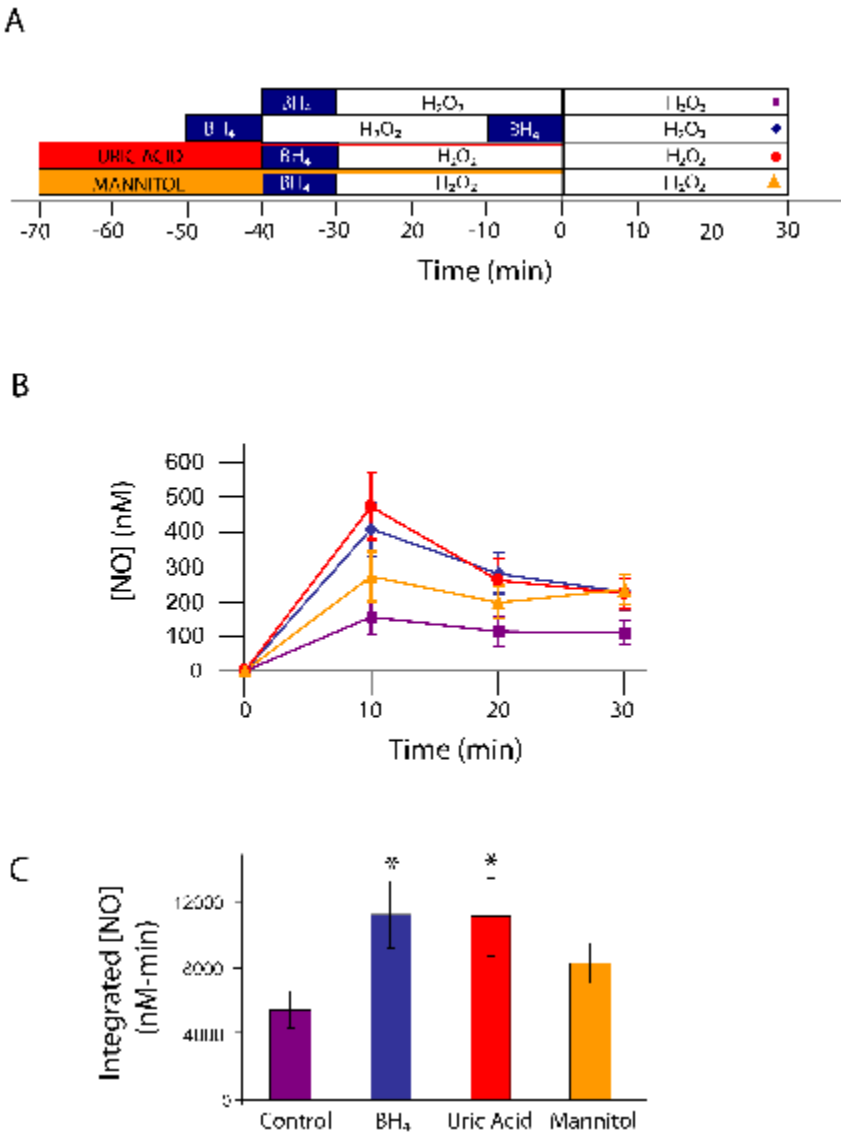

Figure 3-6: $ONOO^-$ and •OH scavengers preserve NO• production after multiple H_2O_2 additions. Panel A: Time course of treatments with $ONOO^-$ scavenger uric acid (100 µM), •OH scavenger mannitol (3 mM), and H_2O_2 (50㎜M). Panel B: Uric acid prevents the reduction in NO• production during H_2O_2 exposure 2, while mannitol partially recovers NO• production during H_2O_2 exposure 2. The time courses of NO• production during H_2O_2 exposure 2 for control (purple squares, n=9), BH_4 (blue diamonds, n=4), urate (red circles, n=4), and mannitol (orange triangles, n=6) are shown. Panel C: Integrated NO• production over 30 min during H_2O_2 exposure 2 indicates that BH_4, uric acid, and mannitol improve NO• bioavailability when compared to control cells. Uric acid treatment resulted in a statistically significant improvement from control (= $p<0.05$) that was indistinguishable from that of BH_4 ($p=0.65$), suggesting that the decrease in NO• bioavailability on second exposure in the control case could be explained by $ONOO^-$-mediated oxidation of BH_4 to create uncoupled eNOS. Mannitol resulted in a partial recovery of NO• bioavailability ($p>0.05$).*

3.5 Discussion

Many disease states are associated with decreased NO• and increased oxidative stress, yet exposure to moderate levels of oxidative stress induces increased NO• production and production capacity[11, 53], presumably compensatory mechanisms. Therefore, it seems likely that some failure of these mechanisms is associated with the progression of disease. One possible mechanism that could explain the transition from compensated to uncompensated states is eNOS uncoupling. In this case, eNOS recruited by moderate levels of oxidative stress would actually contribute to generation of ROS by transferring electrons to molecular oxygen to produce $O_2^{\bullet-}$ rather than to L-arginine to produce NO•. Here, we show that addition of H_2O_2 to BAECs caused an initial increase in NO•. Rechallenging with H_2O_2 caused the increase in NO• production to be attenuated. The decline in H_2O_2-induced NO• production could be mitigated with BH_4 supplementation, suggesting BH_4 oxidation and subsequent uncoupling of eNOS may play a role in the attenuation of the response to H_2O_2.

By itself, H_2O_2 is not very effective at oxidizing BH_4[8, 9]. On the other hand, H_2O_2 activates not only eNOS but also $O_2^{\bullet-}$-producing NADPH oxidase[10]. Furthermore, increased NADPH oxidase activity is associated with hypertension and progression of atherosclerosis, suggesting that this enzyme may be part of the pathogenic cascade that leads to uncompensated oxidative stress in these diseases[11]. Therefore, we tested whether the effect of repeat challenges by H_2O_2 could be mediated by the NADPH oxidase and its product, $O_2^{\bullet-}$. Genetic inhibition of NADPH oxidase in $p47^{phox}$-knockout cells resulted in NO• production that was similar during both H_2O_2 exposures ($p=0.7$). Inhibition of NADPH oxidases by apocynin resulted in a recovery of H_2O_2-induced NO• production to the level seen with BH_4 supplementation ($p=0.96$). Scavenging $O_2^{\bullet-}$ with PEG-SOD had an effect that was statistically indistinguishable from apocynin ($p=0.25$),

although mean NO• production in cells treated with PEG-SOD was higher than in cells treated with apocynin. This trend toward increased NO• in PEG-SOD treated cells could be explained if additional protection from oxidative degradation of NO• was provided by scavenging oxygen radicals from other sources such as xanthine oxidase, cyclooxygenase, cytochrome P450, and mitochondria. Nevertheless, the majority of PEG-SOD effect could be attributed to NADPH oxidase produced $O_2^{\bullet-}$.

Although $O_2^{\bullet-}$ can oxidize BH_4, $ONOO^-$ and •OH are known to be more potent BH_4 oxidizers[8, 9, 45]. Because $ONOO^-$ is formed when $O_2^{\bullet-}$ and NO• react, scavenging of $O_2^{\bullet-}$ would indirectly prevent BH_4 oxidation by $ONOO^-$. Since uric acid scavenging resulted in NO• production statistically similar to that if cells were supplemented a second time with BH_4 ($p=0.97$), the most parsimonious interpretation is that much of the eNOS dysfunction is mediated by the $O_2^{\bullet-}$ downstream product, $ONOO^-$. Scavenging of •OH with mannitol resulted in a partial recovery of NO• production, suggesting it is less important in the overall effect. This could be because •OH is less prevalent in endothelial cells than $ONOO^-$. While there are other possible explanations for the effects of oxygen radicals on eNOS[60, 61], the similarity of BH_4 supplementation with the effects of PEG-SOD, apocynin, and urate, suggests that uncoupling of eNOS by BH_4 oxidation is sufficient to explain the observed reduction in NO• produced with repeat H_2O_2 exposures.

BH_4 oxidation in response to H_2O_2 may be part of the explanation of the failure of oxidative stress compensatory mechanisms. H_2O_2 causes an increase in eNOS production[53]; however, if BH_4 is oxidized, this eNOS may become uncoupled and could contribute to the production of $O_2^{\bullet-}$ [36]. This effect could be counterbalanced by H_2O_2-induced BH_4 production by GTPCH[9], but GTPCH expression has been shown to be decreased in cardiovascular disease states such as diabetes, hypertension, and cardiomyopathy[62-64]. Although the mechanism behind this downregulation remains

unclear, increased BH_4 oxidation coupled with decreased BH_4 production would significantly contribute to the disease state. Therefore, preservation of BH_4 by preventing its oxidation could help to maintain the oxidative stress balance and slow the progression of cardiovascular disease.

Although a direct connection between cell culture and clinical importance is difficult to make, these results suggest two potential clinical treatments that could be used to preserve eNOS function: BH_4 supplementation and NADPH oxidase inhibition. Oral BH_4 has been used as a treatment for mild phenylketonuria in humans[65, 66] and has successfully lowered blood pressure in hypertensive mice[36]. The success of NADPH oxidase inhibition in restoring H_2O_2-induced NO• production is also promising, since NADPH oxidases can be pharmacologically inhibited. Two classes of drugs, statins and angiotensin receptor agonists, have been found to inhibit NADPH oxidase. The actions of these drugs are not specific for NADPH oxidase inhibition. For example, statins can also activate cytochrome P450, which produces $O_2^{\bullet-}$ [24], potentially decreasing the NO• recovery effect. On the other hand, statins have also been shown to increase production of GTP cyclohydrolase I[67], potentially adding to positive NO• recovery effects. Apocynin, a specific inhibitor of NADPH oxidase, has been used in clinical trials in the Netherlands[68] and in herbal medicine[69]. A better understanding of the way NADPH oxidases affect NO• production may reveal additional uses for these drugs.

3.6 Conclusion

Although H_2O_2 causes an initial increase in NO• production, NO• levels decline with additional exposures to H_2O_2. The decline can be prevented by BH_4 supplementation, scavengers of ROS, and NADPH oxidase inhibition. The similarity of these effects suggests that eNOS dysfunction to repeat H_2O_2 exposures can be explained by oxidation of BH_4 by $ONOO^-$ produced when H_2O_2 activates both eNOS and NADPH oxidase.

CHAPTER 4

FUTURE DIRECTIONS

4.1 Introduction

These studies also included many experiments that were not included in the previous chapters because they are preliminary in nature or the results are incompletely understood. They are included here because they represent promising future lines of investigation.

4.2 Possible Role of Dihydrobiopterin in NO• Recovery

As a control experiment, the BH_4 supplementation experiments in chapter 3 were repeated, replacing the second BH_4 supplementation with the more oxidized BH_2 to test whether in the presence of the more oxidized BH_2, the BAEC NO• production would be similar to that in unsupplemented cells. BAECs were cultured as before and incubated for 10 min in 60 µM BH_4, rinsed with PBS, and exposed to 50 µM H_2O_2. Cells were rinsed with PBS and then incubated for 10 min in 60 µM BH_2 before again being exposed to 50 µM H_2O_2. Surprisingly, BH_2 supplementation resulted in partial recovery of NO• release during H_2O_2 exposure 2 (figure 4-1). The easiest explanations for this result are that BH_2 is being converted to BH_4 by dihydrofolate reductase[41] or that BH_2 can act as a oxygen radical scavenger. It may be interesting to study this pathway further to determine why oxidized BH_4 cannot be adequately replenished via the salvage pathway under our experimental conditions. Perhaps more oxidized biopterin would be a better control. Some groups have used (6*S*)-5,6,7,8-tetrahydro-L-biopterin, the

stereoisomer of the cofactor (6*R*)-5,6,7,8-tetrahydro-L-biopterin as a control[70]. The two have the same reducing power, but the S stereoisomer cannot function as a cofactor.

A

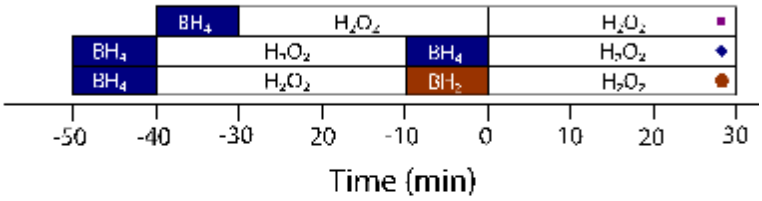

B

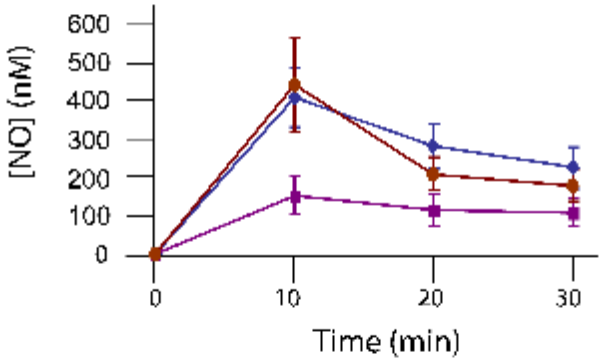

C

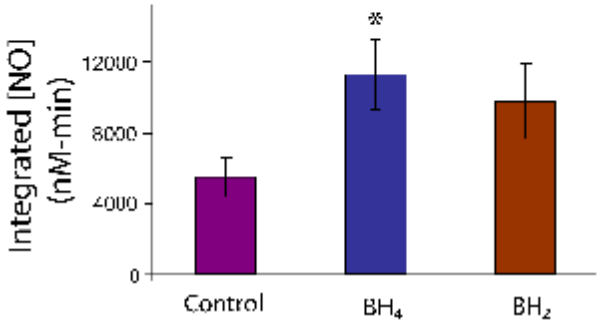

Figure 4-1: Treating cells with BH_2 results in a partial recovery of NO• production. Panel A: Time course for cell treatments BH_4 (60 µM), BH_2 (60 µM), and H_2O_2 (50 µM). Panel B: Comparison of NO• production during H_2O_2 exposure 2. Time courses for control (n=9, purple squares), BH_4 (n=4, blue diamonds), and BH_2 (n=5, brown circles) are shown. Panel C: Integrated NO• production over 30 min during H_2O_2 exposure 2 indicates that BH_2 results in a partial recovery of NO• (p>0.05 as compared to control), suggesting involvement of the 'salvage' pathway of BH_4 production or BH_2 acting as an oxygen radical scavenger.

4.3 Measuring NO• from Cardiac Tissue

As discussed in chapter 2, NO• can be measured electrochemically from cardiac tissue. Multiple attempts were made to measure NO• from the endocardium of hearts excised from pigs with atrial fibrillation (rapid pacing model) and mice with hypertension (DOCA salt model).

Preliminary data comparing NO• production in the hearts of control mice and DOCA hypertensive mice showed a decrease in NO• production in DOCA hearts. This corresponds well to work by Landmesser et al., in which DOCA mice fed tetrahydrobiopterin had improved endothelial function and decreased blood pressure[36]. Because of spatial variability noted in chapter 2, it might prove more convenient to use larger electrodes in this study. This would increase the NO• signal and reduce experimental variability because of microheterogeneity. Continuing experiments begun here will further elucidate the role of oxidative stress in cardiovascular disease.

REFERENCES

1. Irani K. Oxidant Signaling in Vascular Cell Growth, Death, and Survival: A Review of the Roles of Reactive Oxygen Species in Smooth Muscle and Endothelial Cell Mitogenic Apoptotic Signaling. *Circ Res*. 2000;87:179-183.

2. Kojda G, Harrison D. Interactions between NO and reactive oxygen species: pathophysiological importance in atherosclerosis, hypertension, diabetes and heart failure. *Cardiovasc Res*. 1999;43:562-571.

3. Kojda G, Cheng YC, Burchfield J, Harrison DG. Dysfunctional Regulation of Endothelial Nitric Oxide Synthase (eNOS) Expression in Response to Exercise in Mice Lacking One eNOS Gene. *Circulation*. 2001;103:2839-2844.

4. Navarro A, Gomez C, Lopez-Cepero JM, Boveris A. Beneficial effects of moderate exercise on mice aging: survival, behavior, oxidative stress, and mitochondrial electron transfer. *Am J Physiol Regul Integr Comp Physiol*. 2003;286:R505-R511.

5. Napoli C, Williams-Ignarro S, DeNigris F, Lerman LO, Rossi L, Guarino C, Mansueto G, DiTuoro F, Pignalosa O, DeRosa G, Sica V, Ignarro LJ. Long-term combined beneficial effects of physical training and metabolic treatment on atherosclerosis in hypercholesterolemic mice. *Proc Natl Acad Sci USA*. 2004;101:8797-8802.

6. Loscalzo J, Vita JA. Nitric Oxide and the Cardiovascular System. Totowa, NJ: Humana Press; 2000.

7. Stuehr D, Pou S, Rosen GM. Oxygen Reduction by Nitric-oxide Synthases. *J Biol Chem*. 2001;276:14533-14536.

8. Laursen JB, Somers M, Kurz S, McCann L, Warnholtz A, Freeman BA, Tarpey M, Fukai T, Harrison DG. Endothelial Regulation of Vasomotion in ApoE-Deficient Mice: Implications for Interactions between Peroxynitrite and Tetrahydrobiopterin. *Circulation*. 2001;103:1282-1288.

9. Shimizu S, Ishii M, Miyasaka Y, Wajima T, Negoro T, Hagiwara T, Kiuchi Y. Possible involvement of hydroxyl radical on the stimulation of tetrahydrobiopterin synthesis by hydrogen peroxide and peroxynitrite in vascular endothelial cells. *Int J Biochem Cell Biol*. 2005;37:864-875.

10. Cai H, Griendling KK, Harrison DG. The vascular NAD(P)H oxidases as therapeutic targets in cardiovascular diseases. *Trends Pharmacol Sci*. 2003;24:471-478.

11. Cai H, Li Z, Davis ME, Kanner W, Harrison DG, Dudley SC, Jr. Akt-dependent phosphorylation of serine 1179 and mitogen-activated protein kinase kinase/extracellular signal-regulated kinase 1/2 cooperatively mediate activation of the endothelial nitric-oxide synthase by hydrogen peroxide. *Mol Pharmacol*. 2003;63:325-331.

12. Brovkovych V, Stolarczyk E, Oman J, Tomboulian P, Malinski T. Direct electrochemical measurement of nitric oxide in vascular endothelium. *J Pharm Biomedi Anal*. 1999;19:135-143.

13. Malinski T, Czuchajowski L, Feelisch M, Stamler JS. Nitric oxide measurement by electrochemical methods. In: Methods in Nitric Oxide Research. West Sussex, England: John Wiley & Sons Ltd.; 1996. p. 319.

14. Xian Y, Liu M, Cai Q, Li H, Lu J, Jin L. Preparation of microporous aluminium anodic oxide film modified Pt nano array electrode and application in direct measurement of nitric oxide release from myocardial cells. *Analyst*. 2001;126:871-876.

15. Malinski T, Taha Z. Nitric oxide release from a single cell measured in situ by a porphyrinic-based microsensor. *Nature*. 1992;358:676-678.

16. Friedemann MN, Robinson SW, Gerhardt GA. o-Phenylenediamine-modified carbon fiber electrodes for the detection of nitric oxide. *Anal Chem*. 1996;68:2621-2628.

17. Mesaroš Š. Determination of nitric oxide saturated solution by amperometry on modified microelectrode. *Methods Enzymol*. 1999;301:160-168.

18. Moncada S, Radomski MW, Palmer RM. Endothelium-derived relaxing factor. Identification as nitric oxide and role in the control of vascular tone and platelet function. *Biochem Pharmacol*. 1988;37:2495-2501.

19. Ignarro LJ, Buga GM, Byrns RE, Wood KS, Chaudhuri G. Endothelium-derived relaxing factor and nitric oxide possess identical pharmacologic properties as relaxants of bovine arterial and venous smooth muscle. *J Pharmacol Exp Ther*. 1988;246:218-226.

20. Pinsky DJ, Patton S, Mesaroš Š, Brovkovych V, Kubaszewski E, Grunfeld S, Malinski T. Mechanical transduction of nitric oxide synthesis in the beating heart. *Circ Res*. 1997;81:372-379.

21. Cai H, Li Z, Goette A, Mera F, Honeycutt C, Feterik K, Wilcox JN, Dudley SC, Jr., Harrison DG, Langberg JJ. Downregulation of endocardial nitric oxide synthase expression and nitric oxide production in atrial fibrillation: potential mechanisms for atrial thrombosis and stroke. *Circulation*. 2002;106:2854.

22. Lacy F, O'Connor DT, Schmid-Schonbein GW. Plasma hydrogen peroxide production in hypertensives and normotensive subjects at genetic risk of hypertension. *J Hypertens*. 1998;16:291-303.

23. McNeil CJ, Athey D, Ho WO. Direct electron transfer bioelectronic interfaces: application to clinical analysis. *Biosensors & Bioelectronics*. 1995;10:75-83.

24. Li J-M, Shah AM. Endothelial cell superoxide generation: regulation and relevance for cardiovascular pathophysiology. *Am J Physiol Regul Integr Comp Physiol*. 2004;287:R1014-R1030.

25. Spieker LE, Noll G, Ruschitzka FT, Maier W, Luscher TF. Working Under Pressure: the Vascular Endothelium in Arterial Hypertension. *J Hum Hypertens*. 2000;14:617-630.

26. OrtizDeMontellano PR, Nishida C, Rodriguez-Crespo I, Gerber N. Nitric Oxide Synthase Structure and Electron Transfer. *Drug Metab and Dispos*. 1998;26:1185-1189.

27. Sessa WC. eNOS at a glance. *J Cell Sci*. 2004;117:2427-2429.

28. Michell BJ, Griffiths JE, Mitchelhill KI, Rodriguez-Crespo I, Tiganis T, Bovinovski S, deMontellano PR, Kemp BE, Pearson RB. The Akt kinase signals directly to endothelial nitric oxide synthase. *Curr Biol*. 1999;9:845-8.

29. Chen ZP, Mitchelhill KI, Michell BJ, Stapleton D, Rodriguez-Crespo I, Witters LA, Power DA, OrtizdeMontellano PR, Kemp BE. AMP-activated protein kinase phosphorylation of endothelial NO synthase. *FEBS Lett*. 1999;443:285-289.

30. Boo YC, Jo H. Flow-dependent regulation of endothelial nitric oxide synthase: role of protein kinases. *Am J Physiol Cell Physiol*. 2003;285:C499-C508.

31. Wang Y, Nagase S, Koyama A. Stimulatory effect of IGF-I and VEGF on eNOS message, protein expression, eNOS phosphorylation and nitric oxide production in rat glomeruli, and the involvement of PI3-K signaling pathway. *Nitric Oxide*. 2004;10:25-35.

32. Morales-Ruiz M, Lee MJ, Zollner S, Gratton JP, Scotland R, Shiojima I, Walsh K, Hla T, Sessa WC. Spingosine-1-phosphate activates Akt, nitric oxide production, and chemotaxis through a Gi protein/phosphoinositide 3-kinase pathway in endothelial cells. *J Biol Chem*. 2001;276:19672-19677.

33. Hisamoto K, Ohmichi M, Kurachi H, Hayakawa J, Kanda Y, Nishio Y, Adachi K, Tasaka K, Miyoshi E, Fujiwara N, Taniguchi N, Murata Y. Estrogen induces the Akt-dependent activation of endothelial nitric-oxide synthase in vascular endothelial cells. *J Biol Chem*. 2001;276:3459-3467.

34. Bernier SG, Haldar S, Michel T. Bradykinin-regulated interactions of the mitogen-activated protein kinase pathway with the endothelial nitric-oxide synthase. *J Biol Chem*. 2000;275:30707-30715.

35. Berka V, Wu G, Yeh H-C, Palmer G, Tsai A-l. Three Different Oxygen-induced Radical Species in Endothelial Nitric-oxide Synthase Oxygenase Domain under Regulation by L-Arginine and Tetrahydrobiopterin. *J Biol Chem*. 2004;279:32243-32251.

36. Landmesser U, Dikalov S, Price SR, McCann L, Fukai T, Holland SM, Mitch WE, Harrison DG. Oxidation of tetrahydrobiopterin leads to uncoupling of endothelial cell nitric oxide synthase in hypertension. *J. Clin Invest.* 2003;111:1201-1209.

37. Thony B, Ding Z, Martinez A. Tetrahydrobiopterin protects phenylalanine hydroxylase activity in vivo: implications for tetrahydrobiopterin-responsive hyperphenylalaninemia. *FEBS Lett*. 2004;577:507-511.

38. Zeng BY, Heales SJ, Canevari L, Rose S, Jenner P. Alterations in expression of dopamine receptors and neuropeptides in the striatum of GTP cyclohydrolase-deficient mice. *Exp Neurol*. 2004;190:515-524.

39. Thony B, Auerbach G, Blau N. Tetrahydrobiopterin biosynthesis, regeneration and functions. *Biochem J*. 2000;347:1-16.

40. Shi W, Meininger CJ, Haynes TE, Hatakeyama K, Wu G. Regulation of tetrahydrobiopterin synthesis and bioavailability in endothelial cells. *Cell Biochem Biophys*. 2004;41:415-434.

41. Alp NJ, Channon KM. Regulation of Endothelial Nitric Oxide Synthase by Tetrahydrobiopterin in Vascular Disease. *Arterioscler Thromb Vasc Biol*. 2004;24:413-420.

42. Gesierich A, Niroomand F, Tiefenbacher CP. Role of human GTP cyclohydrolase I and its regulatory protein in tetrahydrobiopterin metabolism. *Basic Res Cardiol*. 2003;98:69-75.

43. Nichol CA, Lee CL, Edelstein MP, Chao JY, Duch DS. Biosynthesis of tetrahydrobiopterin by de novo and salvage pathways in adrenal medulla extracts, mammalian cell cultures, and rat brain in vivo. *Proc Natl Acad Sci USA*. 1983;80:1546-1550.

44. Marinos RS, Zhang W, Wu G, Kelly KA, Meininger CJ. Tetrahydrobiopterin levels regulate endothelial cell proliferation. *Am J Physiol Heart Circ Physiol*. 2001;281:H482-H489.

45. Patel KB, Stratford MRL, Wardman P, Everett SA. Oxidation of Tetrahydrobiopterin by Biological Radicals and Scavenging of the Trihydrobiopterin Radical by Ascorbate. *Free Radic Biol Med*. 2002;32:203-211.

46. Taniyama Y, Griendling KK. Reactive Oxygen Species in the Vasculature: Molecular and Cellular Mechanisms. *Hypertension*. 2003;42:1075-1081.

47. Luscher TF, Boulanger CM, Dohi Y, Yang ZH. Endothelium-derived contracting factors. *Hypertension*. 1992;19:117-30.

48. Tsai KL, Wang SM, Chen CC, Fong TH, Wu ML. Mechanism of oxidative stress-induced intracellular acidosis in rat cerebellar astrocytes and C6 glioma cells. *J Physiol*. 1997;502:161-74.

49. McNaught AD, Wilkinson A, editors. IUPAC Compendium of Chemical Terminology: The Gold Book, Second Edition. Second Edition ed. Malden, MA: Blackwell Science, Inc.; 1997.

50. Griendling KK, Sorescu D, Ushio-Fukai M. NAD(P)H Oxidase: Role in Cardiovascular Biology and Disease. *Circ Res*. 2000;86:494-501.

51. Li JM, Shah AM. Mechanism of endothelial cell NADPH oxidase activation by angiotensin II. Role of p47phox subunit. *J Biol Chem*. 2003;278:12094-12100.

52. Stolk J, Hiltermann TJ, Dijkman JH, Verhoeven AJ. Characteristics of the inhibition of NADPH oxidase activation in neutrophils by apocynin, a methoxy-substituted catechol. *Am J Respir Cell Mol Biol*. 1994;11:95-102.

53. Drummond GR, Cai H, Davis ME, Ramasamy S, Harrison DG. Transcriptional and Posttranscriptional Regulation of Endothelial Nitric Oxide Synthase Expression by Hydrogen Peroxide. *Circ Res*. 2000;86:347-354.

54. Jaimes EA, Sweeney C, Raij L. Effects of the Reactive Oxygen Species Hydrogen Peroxide and Hypochlorite on Endothelial Nitric Oxide Production. *Hypertension*. 2001;38:877-883.

55. Al-Baldawi RN. Endothelial nitric oxide synthase function during oxidative stress [Honors Thesis]. Atlanta, GA: Emory University; 2004.

56. Hwang J, Saha A, Boo YC, Sorescu GP, McNally JS, Holland SM, Dikalov S, Giddens DP, Griendling KK, Harrison DG, Jo H. Oscillatory Shear Stress Stimulates Endothelial Production of O2- from p47phox-dependent NAD(P)H Oxidases, Leading to Monocyte Adhesion. *J Biol Chem*. 2003;278:47291-47298.

57. Smith AR, Visioli F, Hagen TM. Vitamin C matters: increased oxidative stress in cultured human aortic endothelial cells without supplemental ascorbic acid. *FASEB J*. 2002;16:1102-1104.

58. Channon KM. Tetrahydrobiopterin regulator of endothelial nitric oxide synthase in vascular disease. *Trends Cardiovasc Med*. 2004;14:323-327.

59. Kuzkaya N, Weissmann N, Harrison DG, Dikalov S. Interactions of peroxynitrite, tetrahydrobiopterin, ascorbic acid, and thiols: implications for uncoupling endothelial nitric-oxide synthase. *J Biol Chem*. 2003;278:22546-22554.

60. Li H, Raman CS, Glaser CB, Blasko E, Young TA, Parkinson JF, Whitlow M, Poulos TL. Crystal structures of zinc-free and -bound heme domain of human inducible nitric-oxide synthase. Implications for dimer stability and comparison with endothelial nitric oxide synthase. *J Biol Chem*. 1999;274:21276-21284.

61. MacMillan-Crow LA, Crow JP, Kerby JD, Beckman JS, Thompson JA. Nitration and inactivation of manganese superoxide dismutase in chronic rejection of human renal allografts. *Proc Natl Acad Sci USA*. 1996;93:11853-11858.

62. Johns DG, Dorrance AM, Tramontini NL, Webb RC. Glucocorticoids Inhibit Tetrahydrobiopterin-Dependent Endothelial Function. *Exp Biol Med*. 2001;226:27-31.

63. Meininger CJ, Marinos RS, Hatakeyama K, Martinez-Zaguilan R, Rojas JD, Kelly KA, Wu G. Impaired nitric oxide production in coronary endothelial cells of the spontaneously diabetic BB rat is due to tetrahydrobiopterin deficiency. *Biochem J*. 2000;349 (Pt 1):353-356.

64. Ohtsuki M, Nomura T, Morimoto S, Hiramitsu S, Uemura A, Kato S, Kato Y, Shiraishi H, Shimokubo J, Yamamoto N, Hishida H. Suppressed expression of GTP cyclohydrolase I mRNA and accelerated expression of inducible nitric oxide synthase mRNA in endomyocardial biopsy specimens from patients with dilated cardiomyopathy. *Clin Chim Acta*. 2005;353:103-107.

65. Fiege B, Ballhausen D, Kierat L, Leimbacher W, Goriounov D, Schircks B, Thony B, Blau N. Plasma tetrahydrobiopterin and its pharmacokinetic following oral administration. *Mol Genet Metabl*. 2004;81:45-51.

66. Matalon R, Koch R, Michals-Matalon K, Moseley K, Surendran S, Tyring S, Erlandsen H, Gamez A, Stevens RC, Romstad A, Moller LB, Guttler F. Biopterin responsive phenylalanine hydroxylase deficiency. *Genet Med*. 2004;6:27-32.

67. Hattori Y, Nakanishi N, Akimoto K, Yoshida M, Kasai K. HMG-CoA reductase inhibitor increases GTP cyclohydrolase I mRNA and tetrahydrobiopterin in vascular endothelial cells. *Arterioscler Thromb Vasc Biol*. 2003;23:176-182.

68. Peters EA, Hiltermann JT, Stolk J. Effect of apocynin on ozone-induced airway hyperresponsiveness to methacholine in asthmatics. *Free Radic Biol Med*. 2001;31:1442-1447.

69. Liu SX, Chiou GC. Effects of Chinese herbal products on mammalian retinal functions. *J Ocul Pharmacol Ther*. 1996;12:377-386.

70. Ihlemann N, Rask-Madsen C, Perner A, Dominguez H, Hermann T, Kober L, Torp-Pedersen C. Tetrahydrobiopterin restores endothelial dysfunction induced by an oral glucose challenge in healthy subjects. *Am J Physiol Heart Circ Physiol*. 2003;285:H875-H882.